

Scanning-tunneling-microscopy and spectroscopy studies of C_{70} thin films on gold substrates

T. Chen, S. Howells, M. Gallagher, and D. Sarid

Optical Sciences Center, University of Arizona, Tucson, Arizona 85721

L. D. Lamb, D. R. Huffman, and R. K. Workman

Department of Physics, University of Arizona, Tucson, Arizona 85721

(Received 27 February 1992; revised manuscript received 25 March 1992)

Thin films of high-purity C_{70} were deposited on polycrystalline gold surfaces and studied by scanning tunneling microscopy (STM) in ultrahigh vacuum. Topographic images reveal initial-stage growth patterns ranging from close packing with a twofold symmetry to random stacking. C_{70} molecules appear oval-shaped, in agreement with the proposed D_{5h} structure of C_{70} . Static orientational disorder is observed in both close-packed and random-stacked regions. The adsorbed C_{70} molecules show the highest STM contrast at bias voltages well below the HOMO-LUMO gap voltage. These and scanning-tunneling-spectroscopy results are discussed and compared with those obtained previously on similarly prepared C_{60} thin films.

The discovery of the condensed form of the fullerenes¹ has aroused tremendous interest in this new form of carbon and in novel materials derived from it.² The research and development efforts have led to the remarkable discovery of superconductivity in doped solids of C_{60} ,³ the observation of unusual electrical transport,⁴ magnetic,⁵ optical,⁶ and mechanical properties⁷ in C_{60} and C_{70} , successful separation and extraction of a number of higher fullerenes⁸ and the fabrications of a variety of fullerene derivatives.⁹⁻¹¹

C_{60} and C_{70} are the two most abundant fullerene molecules. The proposed structure of C_{60} is a strained carbon cage consisting of twenty hexagonal and twelve pentagonal rings, each formed by distorted carbon sp^2 bonds.¹² The structure of C_{70} can be derived from that of C_{60} by, e.g., inserting ten extra carbon atoms in between the two halves of a C_{60} "cut" perpendicularly to one of its fivefold symmetry axes.^{13,14} The resulting structure has a reduced symmetry of D_{5h} , with five nonequivalent carbon sites, in contrast to the I_h structure of C_{60} with all carbon sites being chemically equivalent.

Recent ^{13}C NMR,¹⁵ Raman and IR spectroscopy,¹⁶ and structural studies^{9,10} of high-purity C_{60} and C_{70} samples have provided experimental evidence that is highly compatible with the key expectations for these proposed structures. Real-space images of C_{60} have been obtained using high-resolution microscopy techniques such as scanning tunneling microscopy (STM),¹⁷⁻²¹ atomic force microscopy,²²⁻²⁴ and TEM (Ref. 25) on thin films of high-purity C_{60} and of C_{60}/C_{70} mixtures prepared on metallic,^{17-20,23} semiconductor,²¹ and insulating substrates.²² In this paper we report on the first scanning tunneling microscopy and spectroscopy (STM-S) studies in ultrahigh vacuum (UHV) of high-purity C_{70} thin films deposited on metal surfaces. STM images show extended coverage of C_{70} molecules ranging from packing with a twofold rational symmetry to random-stacking arrangements on polycrystalline gold substrates. A large fraction of the C_{70} molecules appear oval shaped, in agreement with the proposed structure of C_{70} . Static orientational disorder of

C_{70} in these samples is observed. The highest STM contrast was obtained at bias voltages well below the highest occupied molecular orbital-lowest occupied molecular orbital (HOMO-LUMO) gap voltage, indicating a much reduced molecular character of the adsorbed C_{70} .

The high-purity C_{70} sample used in this study was obtained by repeated chromatography of mixed fullerene material produced by a toluene soxhlet extraction of KH carbon.¹ The chromatography was carried out on an alumina column, with elution by toluene and hexane mixtures, as described elsewhere.⁸ Ultraviolet, visible, and IR absorption studies provide an estimate of 95% or higher for the purity of this sample. High-purity polycrystalline gold substrates were annealed at 700-800 °C in air, and then ultrasonically cleaned in ethanol. Controlled amounts of the high-purity C_{70} dissolved in toluene were deposited on the substrates in air and dried in UHV. Auger electron spectroscopy measurements performed on these samples indicated no further contamination, and that such depositions yielded monolayer coverages of C_{70} . Local coverage of C_{70} is inferred from the STM measurements, as described below.

STM-S measurements²⁶ were carried out in a UHV of 1.0×10^{-10} torr. The STM tips were cut from 250- μm -diam Pt-Ir wires, and tested on cleaved 2H-MoS₂ or highly oriented pyrolytic graphite surfaces prior to the experiment. During STM-S data acquisition, the drift rates in x - and y -scan directions were less than ~ 0.5 Å/min, and negligible in the z direction. All STM images presented here are unfiltered.

Displayed in Fig. 1 are two large-area topographic images of a monolayer coverage of C_{70} , showing their packing arrangements on the gold substrates. Images of the same surface areas obtained at opposite bias polarity revealed essentially the same information, except that the molecular contrast was somewhat reduced. The granular character of the background is typical of the polycrystalline gold substrates used in this study and in our previous work on thin films of C_{60} .¹⁹ Close examination of Figs. 1(a) and 1(b) reveals that most C_{70} molecules appear to

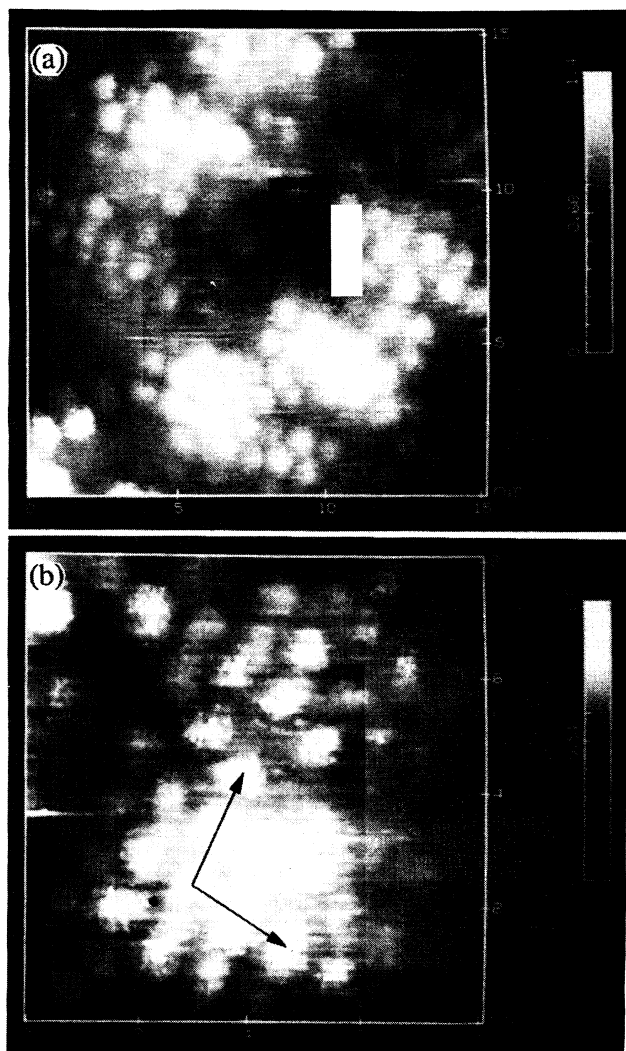


FIG. 1. (a) A topographic image of a monolayer coverage of high-purity C_{70} on a polycrystalline gold substrate, obtained at $V_{\text{bias}} = 73.5$ mV and $I_{\text{tunn}} = 100$ pA, showing both the packing arrangements of monolayer coverage of C_{70} and the morphology of the substrate. (b) Local ordering of C_{70} with a twofold symmetry. The dimensions of C_{70} , as determined from the molecular spacings, are $a = 11 \pm 1$ Å (short axis) and $c = 13 \pm 1$ Å (long axis), yielding an aspect ratio $c/a = 1.2 \pm 0.1$.

be slightly elongated, and the packing in Fig. 1(b) has a twofold symmetry, as indicated by the arrowed lines. The apparent dimensions of these molecules are 11 ± 1 Å along the short axis and 13 ± 1 Å along the long axis, as determined from the molecular spacings in the packed region, yielding an aspect ratio of 1.2 ± 0.1 . Figures 2(a) and 2(d) are topographic images where almost all C_{70} molecules appear oval-shaped. More interestingly, Fig. 2(d) shows a unique packing arrangement that is highly compatible with the structure of C_{70} , and consistent with the twofold symmetry observed in Fig. 1. Note that the thermal drift in the slow-scan direction (vertical) was negligible in all images presented here. This was also verified by comparing the scan-up and scan-down images of the same surface areas. Cross-sectional views of Figs. 2(a) and 2(d) along the solid lines are displayed in Figs.

2(b) and 2(c), and 2(e) and 2(f), respectively. The apparent molecular “height” of 5–8 Å is similar to that of C_{60} on gold obtained under similar imaging conditions.¹⁹ The arrows in Figs. 2(b), 2(c), 2(e), and 2(f), which highlight the molecules, are placed at the molecular “boundaries,” i.e., the locations of local maximum contrast variation. It is interesting to note that the dimensions of these clearly resolved C_{70} molecules, as indicated by these arrows, are rather close to those obtained from the molecular spacings in the packed region. While the overall sizes of the C_{70} in Fig. 2(d) appear slightly larger than that in Fig. 1 due to a looser packing, the aspect ratio of the molecules remains the same.

Tunneling was stable throughout the imaging process. However, mobility of the C_{70} molecules, induced mainly by tip scanning, was indeed observed. This was evidenced by sudden contrast and image changes, which became more frequent as the current setpoint was increased to several nanoamperes. The STM contrast of the adsorbed C_{70} was found to decrease with increasing bias voltage from, e.g., ~ 50 mV (highest contrast) to ~ 800 mV (diminished molecular contrast). This bias-voltage dependence is particularly evident when comparing the dI/dV maps of a same C_{70} coverage area, simultaneously obtained at bias voltages of, e.g., 73.5 and 300 mV (not shown here).

The scanning tunneling spectroscopy results showed the characteristic tunneling spectra ranging from that of a doped semiconductor to an insulator, depending on the local coverage of C_{70} . At monolayer coverage, typical $I-V$ spectra show nearly metallic conductivities at low bias voltages, and an enhanced tunneling at bias voltages above $\pm (0.4-0.6)$ V. $I-V$ spectra which reveal larger energy gaps approaching the full gap of C_{70} were obtained for higher local C_{70} coverages.

As a comparison, our UHV-STM results on high-purity C_{60} thin films on polycrystalline gold substrates reveal that C_{60} molecules pack preferentially in hexagonal arrays, and appear to be spherical in shape, with an average diameter of 11 ± 1 Å, as measured from the molecular spacing in the close-packed regions. The extended hcp arrangement on “rough” polycrystalline gold surfaces reflects the strength of the attractive intermolecular interaction in the initial-stage growth on metal surfaces. The agreement between the measured and expected diameters of C_{60} demonstrates that reliable size measurements can be obtained on fullerene molecules in the close-packed regions based on the periodicity in the STM contrast. There are, however, inherent uncertainties in the size determination of spatially isolated molecules on rough metal surfaces, such as the ones used in these studies. These uncertainties can originate from the tunneling contributions of the inhomogeneous background, often comparable in magnitude to that of the adsorbed molecule, the electronic modifications of the molecule upon adsorption, and the overlap of wave functions in the vicinity of the tip apex. The latter can have significant effects on the STM images of C_{60} and C_{70} , depending on the detailed orbital mixing occurring between the tip apex and the surface area being scanned.

The STM images of high-purity C_{70} thin films prepared

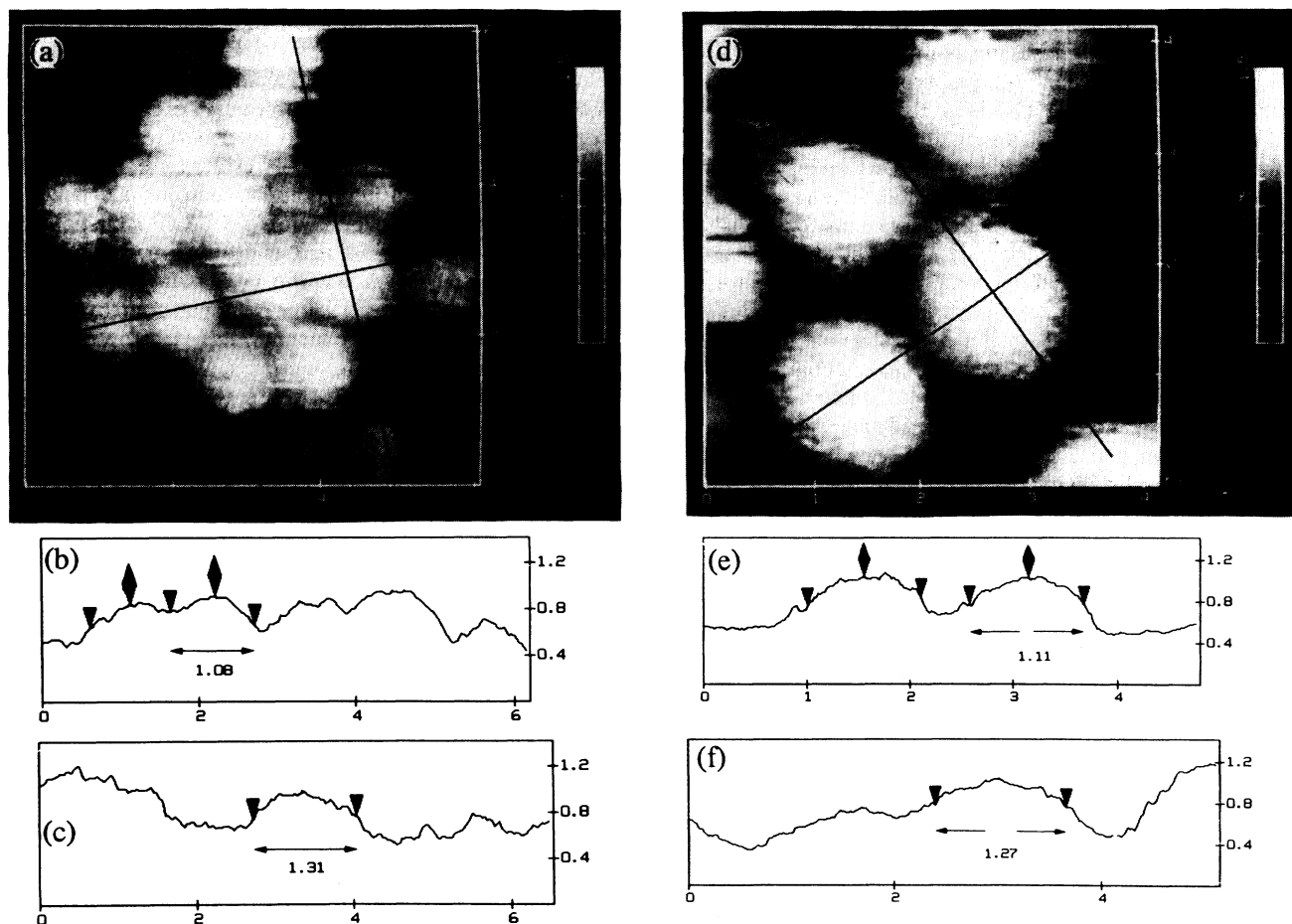


FIG. 2. (a), (d) Topographic images of the oval-shaped C_{70} , and their packing arrangement, as in (d), compatible with the observed twofold symmetry. The solid lines in (a) and (d) indicate the locations for cross-sectional views. (b), (c) and (e), (f) The cross-sectional views of (a) and (d), respectively. The molecular dimensions and their spacings are marked by the arrows and diamonds.

on the same type of gold substrates reveal an overall more disordered initial-stage growth pattern in comparison to that of C_{60} . No hexagonal-closed-packing arrangement is observed for C_{70} at monolayer coverages. A large number of the C_{70} molecules appear elongated, closely matching the proposed D_{5h} structure when viewed perpendicular to its fivefold symmetry axis. While the average dimension of C_{70} along the short axis is found to be $11 \pm 1 \text{ \AA}$, same as the measured diameter of C_{60} , apparent sizes of the long axis show notable variations, especially in the random-stacking regions, due most likely to scattered molecular alignment with respect to the tip axis. The maximum size of the long axis of C_{70} measured in these regions is, however, the same as that obtained from the periodicity in the packed regions shown, e.g., in Fig. 1(b). These measured dimensions and the aspect ratio of $c/a = 1.2 \pm 0.1$ are in good agreement with the expected values of $a \approx 11 \text{ \AA}$, $c \approx 12 \text{ \AA}$, and $c/a \approx 1.1$.²⁷ The "lying-down" position appears to be a preferred adsorption configuration for the C_{70} molecules at monolayer coverage on gold. The apparent molecular height of 5–8 \AA , instead of the expected 11 \AA or larger for C_{70} , may reflect the fact that the wave functions of the delocalized elec-

trons of the gold substrate extend further into the tunneling gap region than that of the adsorbed molecules. The C_{70} molecules, therefore, appear to be partially "embedded" in the gold substrate in the STM topographic images, as shown in Fig. 2.

The observed packing with a twofold symmetry, and the absence of an hcp arrangement of monolayer C_{70} coverage on gold are not surprising in light of the observed oval structure and the apparent absence of molecular rotation. The orientational disorder, as observed in the random stacking and, to a much lesser extent, in the packed regions, appear to be static. The non-hcp arrangement in the absence of dynamic orientational disorder may have important implications to the possible equilibrium bulk crystal structures of C_{70} at, e.g., low temperatures.

The anchoring of the adsorbed C_{70} molecules reflects the chemisorption nature of their attachment to the gold surfaces. This involves the hybridization of the high-lying molecular orbital and energy levels of the gold surface, and a preferential charge transfer from the electron-rich substrate.¹⁹ This mechanism is, in the case of C_{60} adsorbed on gold and platinum surfaces, responsible for the observed intramolecular contrast (IMC). These effects

can be further demonstrated here by the fact that, in our STM studies, the highest contrast of the adsorbed C₆₀ and C₇₀ is obtained at bias voltages typically less than ~0.2 V, well below the HOMO-LUMO gap voltages of 1.7 and 1.6 eV for isolated C₆₀ and C₇₀,²⁸ respectively. In the same bias-voltage range, the *I-V* spectra of the adsorbed C₇₀ molecules display an overall metallic character. The interpretations of these STM observations are consistent with the results of photoemission (PE) studies of C₆₀ and C₇₀ thin films deposited on metal and semiconductor surfaces.²⁹ In particular, the empty-state levels of C₆₀ were found to shift towards the Fermi level by as much as 0.5 eV at a submonolayer coverage, when compared to a higher coverage (> 2 ML) on a gold substrate. This was attributed to a more effective orbital mixing between the first layer C₆₀ and the gold substrate, which produces a LUMO-derived density of states near the Fermi level.²⁹ The anchoring of the fullerene molecules to the gold surfaces is also supported by theoretical considerations based on the attractive interactions between the C₆₀, which become negatively charged upon adsorption, and metal surfaces, and an enhanced covalent bonding of C₆₀ to rough metal surfaces at more reactive sites, such as steps and high-index planes.³⁰

It is interesting to note that, in contrast to C₆₀, IMC is not observed in the adsorbed C₇₀ molecules, despite the absence of thermally induced mobility and rotation. The observed structureless molecular surfaces would imply a higher degree of delocalization of the high-lying π electrons in C₇₀ and/or spinning of C₇₀ about its fivefold symmetry axis, although the latter possibility is highly speculative. While a quantitative analysis is not yet available, a qualitative understanding of the absence of IMC in C₇₀ can be obtained by considering the consequences of the

structural differences between the C₆₀ and the C₇₀, which have direct effects on the high-lying π -electron configurations. Due to its ellipsoidal structure, having five more hexagonal *sp*² rings than does the C₆₀ structure, the surface of C₇₀ is less strained and therefore more graphite-like than that of C₆₀. As a result, an enhancement of the delocalization of high-lying π electrons is expected. In principle this could overshadow subtle effects such as the IMC observed in C₆₀. This trend of a higher degree of π -electron delocalization with an increasing number of hexagonal rings has indeed been demonstrated by recent x-ray absorption near-edge structure,³¹ electron-energy-loss spectroscopy,³² and magnetic susceptibility measurements³³ on high-purity C₆₀ and C₇₀ samples. Under similar imaging conditions and sample preparation, IMC was not observed in the STM images of the "giant" higher fullerenes, which contain as many as 300 carbon atoms.³⁴

In conclusion, our UHV STM-S studies on high-purity C₇₀ thin films deposited on polycrystalline gold substrates directly confirm the proposed structure of C₇₀. The measured molecular dimensions are in good agreement with that expected for the structure. The C₇₀ molecules appear well anchored to the gold substrate at monolayer coverages, and the observed packing arrangement with a two-fold symmetry is highly compatible with the *D*_{5h} symmetry of C₇₀. The observation of significant LUMO-derived density of states near the Fermi level, and the effective anchoring of rough gold surfaces, reflect the consequence of the hybridization between the LUMO orbitals and the energy levels of the gold substrates.

This work was supported by the Air Force Office of Scientific Research and the Office of Naval Research.

¹W. Krätschmer *et al.*, *Nature* (London) **347**, 354 (1990).

²See, for example, *Mater. Res. Soc. Symp. Proc.* **206** (1991).

³A. F. Hebard *et al.*, *Nature* (London) **350**, 600 (1991).

⁴R. C. Haddon *et al.*, *Nature* (London) **350**, 320 (1991).

⁵P.-M. Allemand *et al.*, *Science* **253**, 301 (1991).

⁶W. J. Blau *et al.*, *Phys. Rev. Lett.* **67**, 1423 (1991).

⁷J. E. Fisher *et al.*, *Science* **252**, 1288 (1991).

⁸F. Diederich *et al.*, *Science* **252**, 548 (1991).

⁹J. M. Hawkins *et al.*, *Science* **252**, 312 (1991).

¹⁰P. J. Fagan *et al.*, *Science* **252**, 1160 (1991).

¹¹F. Wudl *et al.*, *Fullerenes* (American Chemical Society, Washington, DC, 1992), Vol. 491.

¹²H. W. Kroto *et al.*, *Nature* (London) **318**, 162 (1985).

¹³H. W. Kroto, *Nature* (London) **329**, 529 (1987).

¹⁴T. G. Schmalz *et al.*, *J. Am. Chem. Soc.* **110**, 1113 (1988).

¹⁵R. Tycko *et al.*, *J. Phys. Chem.* **95**, 518 (1991).

¹⁶D. S. Bethune *et al.*, *Chem. Phys. Lett.* **179**, 181 (1991).

¹⁷R. J. Wilson *et al.*, *Nature* (London) **348**, 621 (1990).

¹⁸J. L. Wragg *et al.*, *Nature* (London) **348**, 623 (1990).

¹⁹T. Chen *et al.*, *Mater. Res. Soc. Symp. Proc.* **206**, 721 (1991);

T. Chen *et al.*, *J. Vac. Sci. Technol. B* **10**, 170 (1992); **9**, 2461 (1991).

²⁰X. P. Gao *et al.* (unpublished).

²¹Y. Z. Li *et al.*, *Science* **253**, 429 (1991).

²²E. J. Snyder *et al.*, *Science* **253**, 171 (1991).

²³D. Sarid *et al.*, *Ultramicroscopy* (to be published).

²⁴P. Dietz *et al.*, *Appl. Phys. Lett.* **60**, 62 (1992).

²⁵Su Wang *et al.*, *Chem. Phys. Lett.* **182**, 1 (1991).

²⁶STM-S measurements were done using a UHV STM from McAllister Technical Services, and a control electronics and computer work station from Digital Instruments, Inc.

²⁷W. Andreoni *et al.*, *Chem. Phys. Lett.* **189**, 241 (1992).

²⁸R. E. Haufler *et al.*, *Chem. Phys. Lett.* (to be published).

²⁹T. R. Ohno *et al.*, *Phys. Rev. B* **44**, 13747 (1991).

³⁰E. Burstein *et al.*, *Phys. Scr.* (to be published).

³¹H. Shinohara *et al.*, *Chem. Phys. Lett.* **183**, 145 (1991).

³²V. P. Dravid *et al.*, *Chem. Phys. Lett.* **185**, 75 (1991).

³³R. C. Haddon *et al.*, *Nature* (London) **350**, 46 (1991).

³⁴L. D. Lamb *et al.*, *Science* **255**, 1414 (1992).

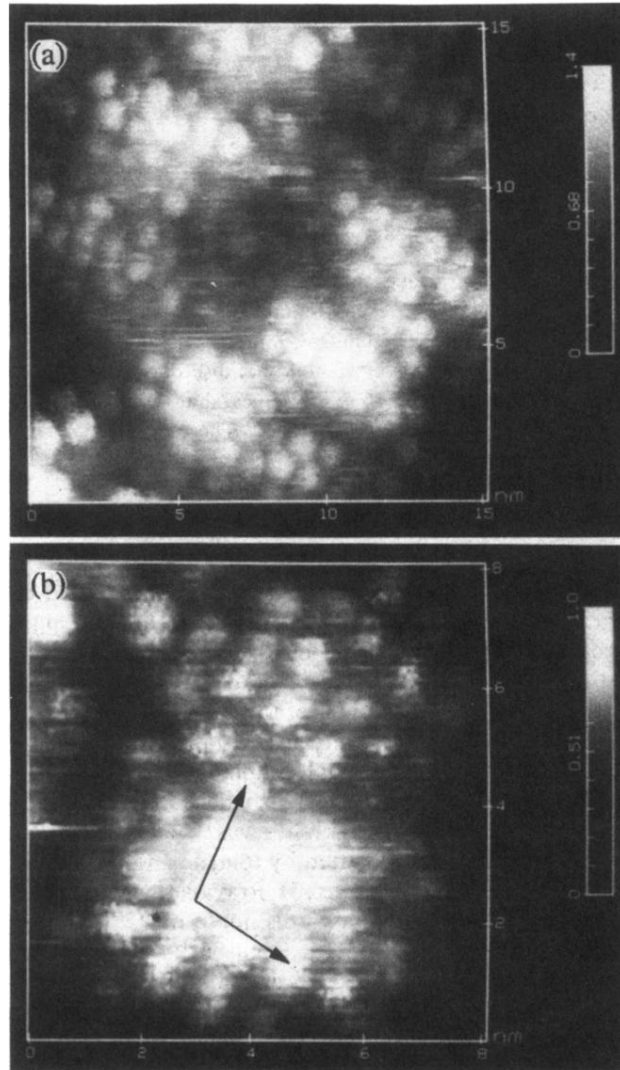


FIG. 1. (a) A topographic image of a monolayer coverage of high-purity C_{70} on a polycrystalline gold substrate, obtained at $V_{\text{bias}} = 73.5$ mV and $I_{\text{tunn}} = 100$ pA, showing both the packing arrangements of monolayer coverage of C_{70} and the morphology of the substrate. (b) Local ordering of C_{70} with a twofold symmetry. The dimensions of C_{70} , as determined from the molecular spacings, are $a = 11 \pm 1$ Å (short axis) and $c = 13 \pm 1$ Å (long axis), yielding an aspect ratio $c/a = 1.2 \pm 0.1$.

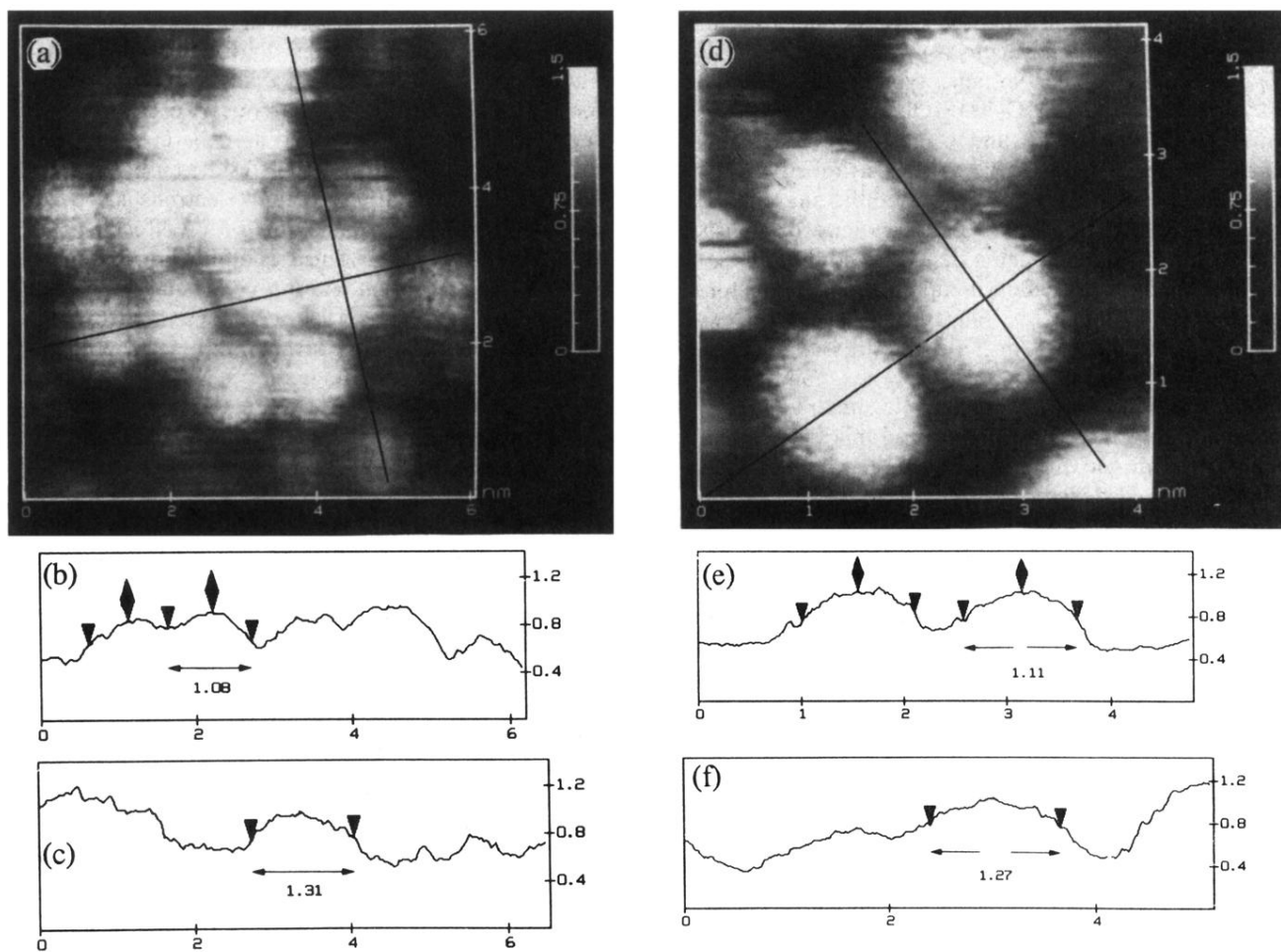


FIG. 2. (a), (d) Topographic images of the oval-shaped C_{70} , and their packing arrangement, as in (d), compatible with the observed twofold symmetry. The solid lines in (a) and (d) indicate the locations for cross-sectional views. (b), (c) and (e), (f) The cross-sectional views of (a) and (d), respectively. The molecular dimensions and their spacings are marked by the arrows and diamonds.